Lanthanide Silicates

DOI: 10.1002/anie.200602849

Optical Detection of Solid-State Chiral Structures with Unpolarized Light and in the Absence of External Fields**

*Duarte Ananias, Filipe A. Almeida Paz, Luís D. Carlos, Carlos F. G. C. Geraldes, and João Rocha**

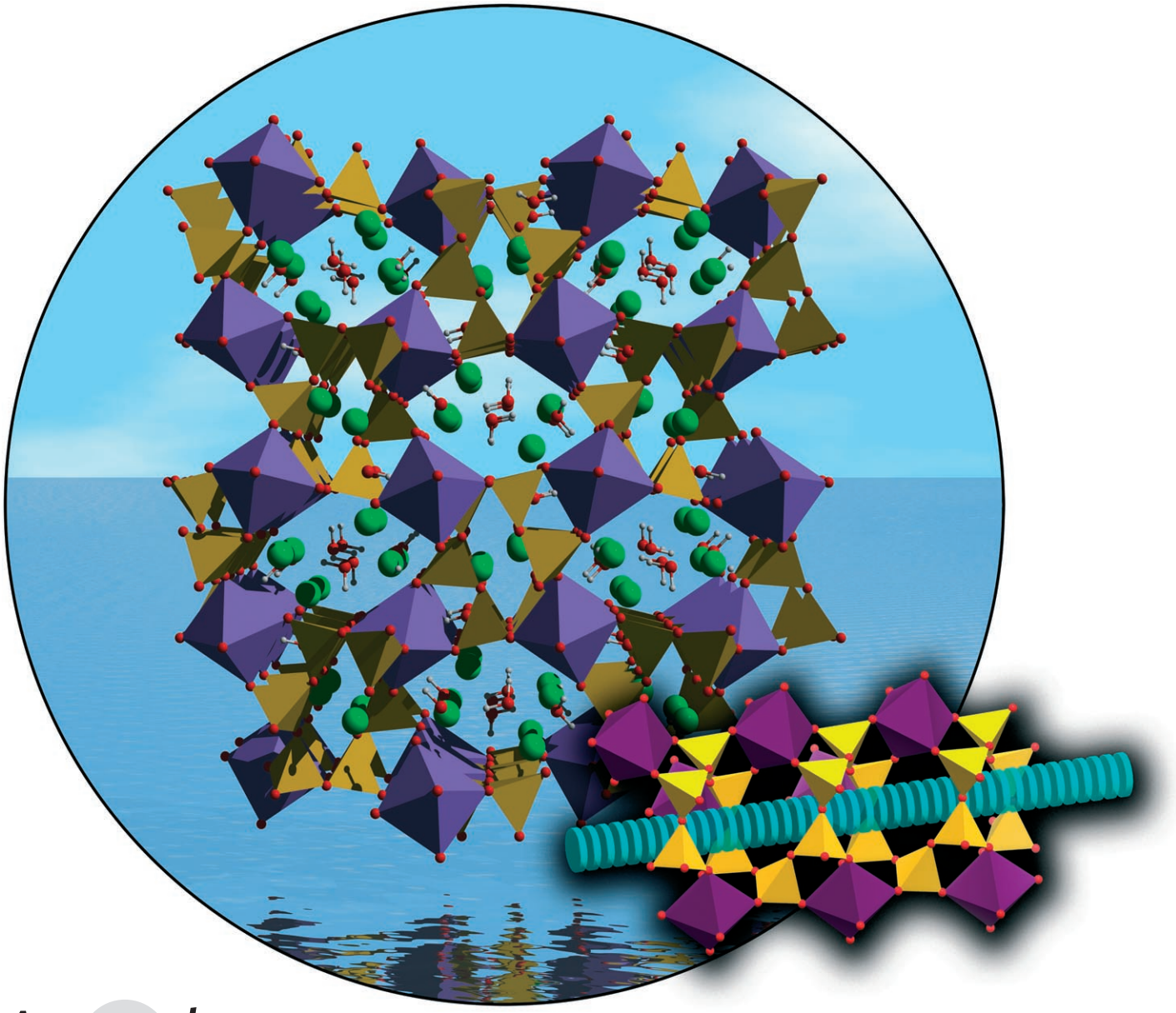

Zeolites are microporous aluminosilicate materials of considerable industrial importance because they are excellent molecular sieves, ion exchangers, and heterogeneous catalysts. With the advent of the nanotechnology era, and increasing interest in the use of molecular sieves for device applications, novel zeolite-type materials containing stoichiometric amounts of lanthanide (Ln) metals that exhibit photoluminescence and magnetic properties have been investigated.[1–3] Herein we report the remarkable framework of $Na_3[(Y,Ln)Si_3O_9]\cdot 3H_2O$ (Ln = Eu, Tb, Er, Ce), an unprecedented chiral, photoluminescent, and microporous Ln–silicate system. Only two zeolite-type silicates exhibit chiral polymorphism, namely zeolite beta and ETS-10, but neither of these materials is photoluminescent.[4,5] The crystal structure of $Na_3[(Y,Ln)Si_3O_9]\cdot 3H_2O$ materials displays $(Si_3O_9)_\infty$ chiral spirals interconnected by $\{(Y,Ln)O_6\}$ octahedra, and it exhibits a statistical excess of one enantiomer over the other. For the first time, we show that Eu^{3+} photoluminescence spectroscopy with excitation by unpolarized light in the absence of an external magnetic field is able to identify, and possibly quantify, enantiomeric domains in chiral frameworks. This enantioselectivity phenomenon may be of importance in the context of fundamental interactions between light and condensed matter.

Although conventional zeolites are built up of tetrahedral $\{SiO_4\}$ and $\{AlO_4\}$ units, microporous silicates whose frameworks contain transition-metal heteropolyhedra have been known since the early 1990s.[1–3] The most prominent member of this family is titanosilicate ETS-10, which contains $\{TiO_6\}$ and $\{SiO_4\}$ units.[5] The constituent elements of heteropolyhedral silicates have been recently extended to lanthanides, and thus properties such as photoluminescence and magnetism have been explored. However, so far only a handful of microporous (stoichiometric) lanthanide silicates are known.[2]

Previously, chirality involving lanthanide complexes has been sensed by magnetochiral dichroism (MChD)[6,7] and circular dichroism (CD) methods, such as Ln-centered absorption, ligand absorption, and Ln-centered circularly polarized luminescence (CPL).[8,9] Whereas CPL measures the difference in emission intensity between left and right circularly polarized light, MChD evaluates the difference in luminescence intensity in the directions parallel and antiparallel to an externally applied magnetic field using unpolarized light (e.g., from a Hg-discharge lamp). Enantiodiscrimination typically uses the magnetic dipole-allowed $Eu(^5D_0\rightarrow{}^7F_1)$, $Tb(^5D_4\rightarrow{}^7F_5)$, and $Yb(^5F_{5/2}\rightarrow{}^2F_{7/2})$ transitions in CPL experiments, whereas in MChD the $^5D_0\rightarrow{}^7F_{1,2}$ transitions are employed.[6–9]

The solids described herein were obtained as byproducts in the hydrothermal synthesis of dense $Na_3[LnSi_3O_9]$ phosphors.[10–12] Crystals suitable for single-crystal X-ray diffraction were prepared for small-pore materials $Na_3[(Y_{0.9}Tb_{0.04}Eu_{0.025}Ce_{0.035})Si_3O_9]\cdot 3H_2O$ (**1a**) and $Na_3[(Y_{0.995}Er_{0.005})Si_3O_9]\cdot 3H_2O$ (**1b**). Isostructural $Na_3[(Y_{0.7}Eu_{0.3})Si_3O_9]\cdot 3H_2O$ (**1c**) and $Na_3[(Y_{0.70}Tb_{0.30})Si_3O_9]\cdot 3H_2O$ (**1d**) were also synthesized as powders and used in the photoluminescence studies. These solids are chiral orthorhombic phases exhibiting a statistical enantiomeric excess (see the Supporting Information). A second type of smaller, monoclinic, centrosymmetric crystals which often cocrystallize with **1**, namely, $H_{0.5}Na_{2.5}[(Y_{0.995}Er_{0.005})Si_3O_9]\cdot 3H_2O$ (**2**), were manually harvested and analyzed on a rotating-anode diffractometer.

The structure of dense $Na_3[LnSi_3O_9]$ is constructed from complex double spiral chains $(Si_{24}O_{72})_\infty$ with a period of 15.14 Å, which connect isolated $\{LnO_6\}$ octahedra.[10] The chiral (**1**) and centrosymmetric (**2**) materials share a common type of $(Si_3O_9)_\infty$ chain (Figure 1b and Supporting Information) running along the [100] direction (period of one *a*-axis length, ca. 6.97 Å). Although the $(Si_{24}O_{72})_\infty$ and $(Si_3O_9)_\infty$ chains are different they are both built up of triortho groups Si_3O_{10}, and the latter chain readily transforms into the former on calcining solids **1** and **2** at 800 °C. We speculate that the Si_3O_{10} group is the structural motif that first forms in the gel and templates the synthesis of the three phases. The silicon oxide chains not only connect individual $\{LnO_6\}$ octahedra but they also isolate them, at minimal Ln···Ln distances of about 6.32 and 5.88 Å in **1** and **2**, respectively (Figure 1 and Supporting Information1). Such separation of the optically active centers is important because it effectively avoids self-quenching.

Although the $(Si_3O_9)_\infty$ structural motif is similar for both **1** and **2**, the way it is linked to the metal centers is different. Consider the first coordination sphere of the $\{(Y,Ln)O_6\}$ distorted octahedra (see the Supporting Information): whereas in **1** chelation of the metal center by three Si_2O_7 moieties ultimately leads to a chiral structure, in **2** one of the chelate rings is broken. As a result, the small-pore structure of the former contains one-dimensional mixed 8-ring channels along the [100] direction, which have a cross section of about 2.0×4.0 Å (Figure 1a) and host Na^+ ions and hydrogen-bonded water molecules, whereas the comparatively dense framework of the latter has 6-ring tunnels housing Na^+ and H^+ ions and water molecules (see the Supporting Information).

[*] Dr. D. Ananias, Dr. F. A. Almeida Paz, Prof. J. Rocha
Departamento de Química
CICECO
Universidade de Aveiro
3810-193 Aveiro (Portugal)
Fax: (+351) 234-370-730
E-mail: rocha@dq.ua.pt
Prof. L. D. Carlos
Departamento de Física
CICECO
Universidade de Aveiro
3810-193 Aveiro (Portugal)
Dr. D. Ananias, Prof. C. F. G. C. Geraldes
Departamento de Bioquímica
Universidade de Coimbra
3001-401 Coimbra (Portugal)

[**] We thank the Portuguese Foundation for Science and Technology (FCT), POCTI, and FEDER, FAME NoE for financial support of this work.

Supporting information for this article is available on the WWW under http://www.angewandte.org or from the author.

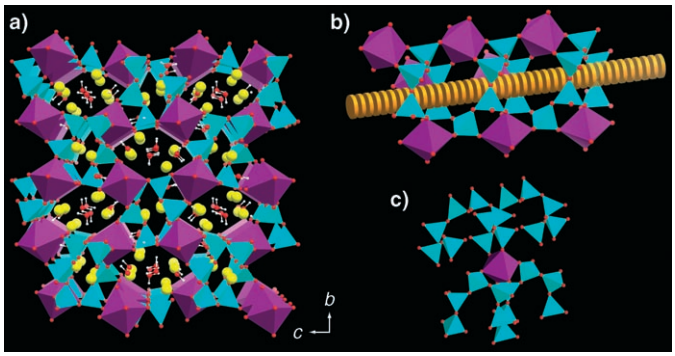

Figure 1. a) Perspective view along the [100] direction of the crystal packing of **1a** and **1b**. b) Portion of the anionic frameworks showing one $(Si_3O_9)_\infty$ spiral chain interconnecting individual $\{(Y,Ln)O_6\}$ octahedra (Ln = Tb^{3+}, Ce^{3+}, Eu^{3+}, or Er^{3+}). c) Idealized representation of a $\{(Y,Ln)O_6\}$ octahedron connected to two $(Si_3O_9)_\infty$ spirals with opposite handedness. Color code: purple $\{(Y,Ln)O_6\}$; blue $\{SiO_4\}$; red O^{2-}; yellow Na^+; white H.

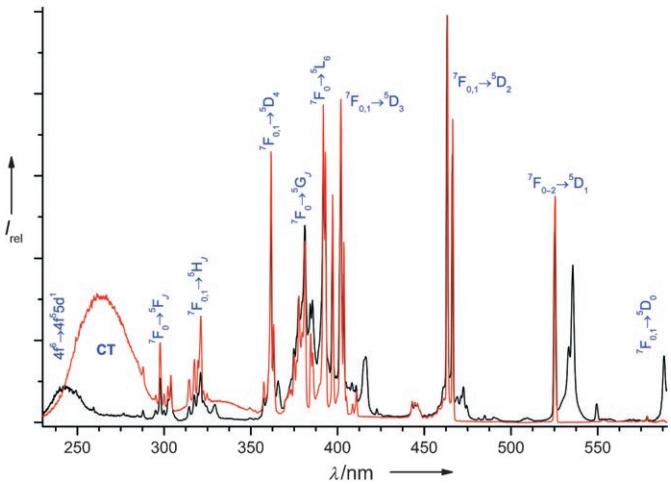

Figure 2. Excitation spectra of **1c** recorded at room temperature (black line) and 10 K (red line). Emission was monitored at 607.2 nm.

Excitation and emission spectra of **1d** were recorded at room temperature and 10 K (Supporting Information). In the excitation spectra, the sharp lines between 280 and 500 nm are assigned to $^7F_6 \rightarrow ^5D_{4-0}$, $^5L_{10}$, $^5G_{6-3}$, $^5H_{7-4}$, and $^5F_{5,4}$ intraconfigurational forbidden $4f^8 \rightarrow 4f^8$ transitions of Tb^{3+}. The broad band between 250 and 280 nm is ascribed to the spin-forbidden (high-spin, HS) interconfigurational $4f^8 \rightarrow 4f^75d^1$ transition of Tb^{3+} (see reference [13] and references therein). This type of spin-forbidden fd band may be observed for (heavy) Ln^{3+} ions with more than seven 4f electrons at an energy lower than that of spin-allowed (low-spin, LS) fd transitions. The broad band at about 236 nm is assigned to the spin-allowed (LS) interconfigurational fd transition of Tb^{3+}. The emission spectra of **1d**, excited at 265 nm, show a series of sharp lines between 475 and 700 nm, assigned to the $^5D_4 \rightarrow ^7F_J$ ($J = 6$–1) transitions of Tb^{3+} (see the Supporting Information). The same emission is obtained with excitation at the intra-$^5D_3$ (377 nm) line.

The excitation spectra of **1c** recorded at room temperature and 10 K (Figure 2) display a series of sharp lines assigned to the $^7F_{0-2} \rightarrow ^5D_{4-0}$, $^5L_6$, $^5G_{2-6}$, $^5H_{3-7}$, and $^5F_{1-5}$ Eu^{3+} intra-$4f^6$ transitions. The faint broad band ($4f^6 \rightarrow 4f^55d^1$) at high energy is probably the beginning of the spin-allowed, interconfigurational fd Eu^{3+} transition band, which normally appears at higher energy than the equivalent Tb^{3+} band. At 10 K the spectrum exhibits an additional broad band that peaks at 264.5 nm and is attributed to ligand-to-Eu^{3+} charge transfer (CT). The energy (4.69 eV) and full-width at half-maximum (0.58 eV) of the CT band are in the range of values reported for many structures containing Eu^{3+}.[14]

The sharp lines of the emission spectra (Figure 3) are assigned to transitions between the first excited nondegenerate $^5D_0$ state and the $^7F_{0-4}$ levels of the fundamental Eu^{3+} septet. Local-field splitting of the $^7F_{1,2}$ levels into three and five Stark components (inset in Figure 3, green line) supports the presence of a single low-symmetry Eu^{3+} environment, as indicated by the crystal structure. Surprisingly, when the sample is excited at the CT band (265 nm) the number of $^7F_{1,2}$ Stark components doubles (inset in Figure 3, magenta line).

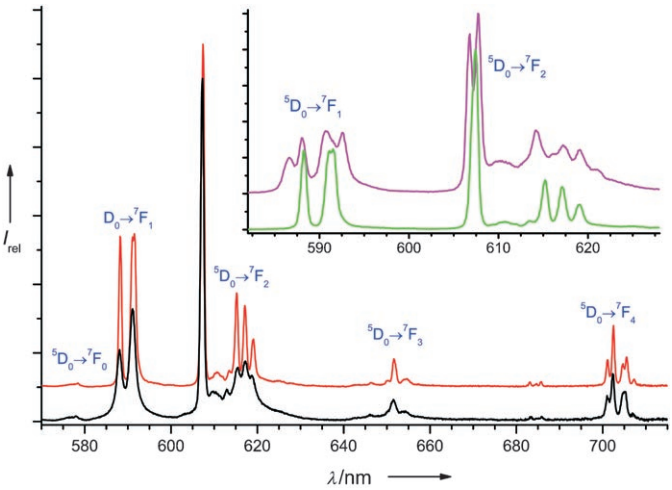

Figure 3. Emission spectra of **1c** recorded at room temperature (black line) and 10 K (red line). Excitation was performed at 525.4 nm. The inset shows an expansion of the Eu^{3+} $^5D_0 \rightarrow ^7F_{1,2}$ transitions, collected at 10 K and excited at 526 nm for the $^5D_1$ level of Eu^{3+} (green line) and at 265 nm for the CT band (magenta line).

We note that this is only observed between 10 and about 120 K, the temperature range in which the CT band is also detected (despite the fact that the X-ray data, collected at 100 K, call for the presence of a single Eu^{3+} site).

Because the $^5D_0 \rightarrow ^7F_0$ line is very faint, we did not draw any conclusions from its evolution when the excitation wavelength was varied from the CT to the intra-4f lines. The relative intensities of the two main $^5D_0 \rightarrow ^7F_2$ Stark components depend on the particular sample studied (see the Supporting Information). This observation constitutes first (though not unequivocal) evidence for the presence of two enantiomers in **1c**. Moreover, the enantioselective detection of Eu^{3+}-containing molecular compounds by CPL and MChD has been found to be much more sensitive in the magnetic dipole-allowed $^5D_0 \rightarrow ^7F_1$ transition than in the induced electric-dipole $^5D_0 \rightarrow ^7F_2$ transition.[6,8,9] In **1c** we observe maximum splittings of the $^5D_0 \rightarrow ^7F_1$ transition of 172 and

95 cm^{-1}, respectively for excitation at the CT band and intra-$4f^6$ lines (inset in Figure 3). For the $^5D_0 \rightarrow {}^7F_2$ transition the maximum splittings are 373 and 310 cm^{-1}, respectively, for the same excitations. Thus, the maximum splitting difference is significantly larger for the $^5D_0 \rightarrow {}^7F_1$ transition (77 cm^{-1}, compared with 63 cm^{-1} for the other transitions).

Measurements of $^5D_0$ lifetimes for $Na_3[(Y_{1-a}Eu_a)Si_3O_9]\cdot 3H_2O$ ($a = 0.2$, 0.3; see the Supporting Information) clearly support this conclusion. In all measurements, the $^5D_0$ decay curves are well fitted by a single exponential (Supporting Information). At 10 K the two samples display a similar lifetime ((1.59 ± 0.01) ms) for excitation in the $^5D_1$ level (526 nm) and detection in the strongest $^7F_2$ Stark component (608.5 nm). However, excitation in the CT band leads to different lifetimes. Whereas the sample with $a = 0.2$ has the same lifetime for the two main $^7F_2$ Stark components at 607.8 and 609.1 nm ((1.48 ± 0.01) ms), that with $a = 0.3$ displays different lifetimes of (1.39 ± 0.01) and (1.54 ± 0.01) ms for detection at these wavelengths, respectively.

We now try to rationalize the unusual detection of enantiomeric domains by photoluminescence spectroscopy with excitation by unpolarized light and in the absence of an external applied magnetic field. Consider Figure 1c: Structurally, the Y^{3+}/Eu^{3+} ions link in different ways to two adjacent $(Si_3O_9)_\infty$ spiral chains which, for the sake of argument, we assume to be enantiomeric. Each Y^{3+}/Eu^{3+} octahedron shares four corners with a spiral of a given handedness, and two corners with a spiral of opposite handedness.

When the material is excited on the CT band, expansion of the Eu^{3+}–O bonds of the two adjacent enantiomeric spirals gives rise to two discernible Eu^{3+} local environments. Indeed, a CT transition involves considerable reorganization of the charge density distribution around the Eu^{3+} ion, which is accompanied by expansion of the Eu^{3+}–O bonds in the excited state.[15] The above-mentioned decrease in the $^5D_0$ lifetime for CT excitation (Supporting Information) lends support to this Eu^{3+}–O expansion. Moreover, as the two main $^5D_0 \rightarrow {}^7F_2$ transitions of the sample with $a = 0.2$ exhibit similar intensities and lifetimes, this material does not contain a significant enantiomeric excess. In contrast, the emission spectrum of the sample with $a = 0.3$ suggests a small enantiomeric excess, slight difference in intensity of the two lines, and distinct lifetimes (see the Supporting Information). Further work is in progress to fully understand the intriguing phenomenon of domain enantioselectivity in microporous framework silicates by photoluminescence spectroscopy.

In conclusion, to the best of our knowledge, discrimination between enantiomeric domains has so far only been achieved by using CPL or MChD.[6–9] Our results raise the exciting possibility that Eu^{3+} photoluminescence spectroscopy may, at least in certain cases, be used to detect, and possibly quantify, enantiomeric domains in chiral frameworks.

Experimental Section

The syntheses of rare-earth-metal silicates were carried out in teflon-lined autoclaves under static hydrothermal conditions in ovens preheated to 150–230 °C. All lanthanide salts were of 99.9 % purity. In all the syntheses, autoclaves were removed and quenched in cold water after an appropriate time. The obtained microcrystalline powders were filtered, washed at room temperature with distilled water, and dried at 100 °C.

Typical synthesis of single crystals of **1a**: An alkaline solution was made by mixing sodium silicate solution (6.83 g, 27 wt % SiO_2, 8 wt % Na_2O, Merck), H_2O (10.07 g), and NaOH (6.59 g, Panreak). A mixture of $YCl_3\cdot 6H_2O$ (1.05 g, Aldrich), $TbCl_3\cdot 6H_2O$ (0.058 g, Aldrich), $EuCl_3\cdot 6H_2O$ (0.035 g, Aldrich), and $CeCl_3\cdot 7H_2O$ (0.050 g, Aldrich) in H_2O (10.0 g) was added to this solution, and the solution was stirred thoroughly. The gel, with composition $2.97\,Na_2O{:}1.00\,SiO_2{:}0.057\,Y_2O_3{:}0.0021\,Tb_2O_3{:}0.0014\,Eu_2O_3{:}0.0014\,Ce_2O_3{:}36.3\,H_2O$, was heated in autoclaves (volume 37 cm^3) for 8 d at 230 °C. The resulting sample also contained single crystals of **2** and dense $Na_3[(Y_{0.9}Tb_{0.04}Eu_{0.025}Ce_{0.035})Si_3O_9]$ (Supporting Information).[10–12]

Typical synthesis of single crystals of **2**: An alkaline solution was made by mixing sodium silicate solution (7.91 g, 27 wt % SiO_2, 8 wt % Na_2O, Merck), H_2O (12.20 g), and NaOH (7.72 g, Panreak). A mixture of $YCl_3\cdot 6H_2O$ (1.293 g, Aldrich) and $ErCl_3\cdot 6H_2O$ (0.008 g, Aldrich) in H_2O (10.0 g) was added to this solution and the solution was stirred thoroughly. The gel, with composition $3.00\,Na_2O{:}1.00\,SiO_2{:}0.060\,Y_2O_3{:}0.0003\,Er_2O_3{:}34.7\,H_2O$, was heated in autoclaves (volume 42 cm^3) for 5 d at 230 °C. The resulting sample also contains small amounts of **1b** and dense $Na_3[(Y_{0.995}Er_{0.005})Si_3O_9]$.[10–12] Ultrasonication of a water suspension of the material disperses the crystals of **2**. Unlike the dense material[10–12] and **1b** crystals, crystals of **2** remain in the aqueous phase and are easily isolated.

Pure samples of **1c** and **1d** were prepared from a similar initial gel by introducing the desired Y^{3+} and Eu^{3+} or Tb^{3+} contents and heating for 13 d at 150 °C (see the Supporting Information).

The chemical composition of the samples was ascertained by energy-dispersive X-ray spectroscopy. Thermogravimetry confirmed that materials **1** and **2** contain three water molecules per formula unit.

Further details on the crystal structure investigations may be obtained from the Fachinformationszentrum Karlsruhe, 76344 Eggenstein-Leopoldshafen, Germany (fax: (+49) 7247-808-666; e-mail: crysdata@fiz-karlsruhe.de), on quoting the depository numbers CSD-415853 (**1a**), -415852 (**1b**), and -415852 (**2**). See also the Supporting Information.

Crystal data for **1a**: $H_{24}Ce_{0.14}Eu_{0.10}Na_{12}O_{48}Si_{12}Tb_{0.16}Y_{3.60}$, $M = 1785.47$, orthorhombic, space group $P2_12_12_1$, $Z = 1$, $a = 6.9724(14)$, $b = 11.687(2)$, $c = 13.404(3)$ Å, $V = 1092.2(4)$ Å^3, $\mu(Mo_{K\alpha}) = 5.864$ mm^{-1}, $\rho_{calcd} = 2.715$ $g\,cm^{-3}$. Of a total of 10557 reflections collected, 2408 were independent ($R_{int} = 0.0525$). Crystal size $0.08 \times 0.07 \times 0.04$ mm. Final $R1 = 0.0288$ [$I > 2\sigma(I)$] and $wR2 = 0.0650$ (all data).

Crystal data for **1b**: $H_{24}Er_{0.02}Na_{12}O_{48}Si_{12}Y_{3.98}$, $M = 1762.36$, orthorhombic, space group $P2_12_12_1$, $Z = 1$, $a = 6.9610(14)$, $b = 11.669(2)$, $c = 13.375(3)$ Å, $V = 1086.4(4)$ Å^3, $\mu(Mo_{K\alpha}) = 5.892$ mm^{-1}, $\rho_{calcd} = 2.694$ $g\,cm^{-3}$. Of a total of 9102 reflections collected, 2226 were independent ($R_{int} = 0.0453$). Crystal size $0.10 \times 0.09 \times 0.06$ mm. Final $R1 = 0.0268$ [$I > 2\sigma(I)$] and $wR2 = 0.0566$ (all data).

Crystal data for **2**: $H_{26}Er_{0.02}Na_{10}O_{48}Si_{12}Y_{3.98}$, $M = 1718.40$, monoclinic, space group $P2_1/n$, $Z = 1$, $a = 9.073(4)$, $b = 8.823(4)$, $c = 12.963(5)$ Å, $\beta = 107.68(2)°$, $V = 988.8(7)$ Å^3, $\mu(Mo_{K\alpha}) = 13.675$ mm^{-1}, $\rho_{calcd} = 2.886$ $g\,cm^{-3}$. Of a total of 2571 reflections collected, 990 were independent ($R_{int} = 0.1025$). Crystal size $0.05 \times 0.05 \times 0.01$ mm^3. Final $R1 = 0.0882$ [$I > 2\sigma(I)$] and $wR2 = 0.2095$ (all data).

Photoluminescence measurements were performed on a Fluorolog-3 Model FL3-2T with double excitation spectrometer (Triax 320), fitted with a 1200-grooves mm^{-1} grating blazed at 330 nm, and a single emission spectrometer (Triax 320), fitted with a 1200-grooves mm^{-1} grating blazed at 500 nm, coupled to an R928P photomultiplier. The excitation source was a 450-W xenon lamp. Excitation

spectra were corrected from 240 to 600 nm for the spectral distribution of the lamp intensity by using a photodiode reference detector. Emission and excitation spectra, recorded between 10 K and room temperature in 20–30-K steps by using a closed-cycle He cryostat, were also corrected for the spectral response of the monochromators and the detector by using typical correction spectra provided by the manufacturer. Time-resolved measurements were carried out with a 1934D3 phosphorimeter coupled to the Fluorolog-3 and a Xe–Hg flash lamp (6 μs/pulse half width and tail of 20–30 μs) was used as excitation source.

Received: July 17, 2006
Revised: September 11, 2006
Published online: October 19, 2006

Keywords: hydrothermal synthesis · lanthanides · luminescence · microporous materials · silicates

[1] J. Rocha, M. W. Anderson, *Eur. J. Inorg. Chem.* **2000**, 801 – 818.
[2] J. Rocha, Z. Lin, *Reviews in Mineralogy and Geochemistry, Vol. 57* (Eds.: G. Ferraris, S. Merlino), Mineralogical Society of America, Geochemical Society, **2005**, chap. 6, pp. 173 – 201.
[3] M. Tsapatsis, *AIChE J.* **2002**, *48*, 654 – 660.
[4] J. M. Newsham, M. M. J. Treacy, W. T. Koetsier, C. B. De Gruyter, *Proc. R. Soc. London Ser. A* **1988**, *420*, 375 – 405.
[5] M. W. Anderson, O. Terasaki, T. Ohsuna, A. Philippou, S. P. Mackay, A. Ferreira, J. Rocha, S. Lidin, *Nature* **1994**, *367*, 347 – 351.
[6] G. L. J. A. Rikken, E. Raupach, *Nature* **1997**, *390*, 493 – 494.
[7] F. S. Richardson, J. P. Riehl, *Chem. Rev.* **1977**, *77*, 773 – 792.
[8] J. P. Riehl, F. S. Richardson, *Chem. Rev.* **1986**, *86*, 1 – 16.
[9] J.-C. G. Bünzli, C. Piguet, *Chem. Soc. Rev.* **2005**, *34*, 1048 – 1077.
[10] D. Ananias, J. P. Rainho, A. Ferreira, M. Lopes, C. M. Morais, J. Rocha, L. D. Carlos, *Chem. Mater.* **2002**, *14*, 1767 – 1772.
[11] D. Ananias, A. Ferreira, L. D. Carlos, J. Rocha, *Adv. Mater.* **2003**, *15*, 980 – 985.
[12] D. Ananias, L. D. Carlos, J. Rocha, *Opt. Mater.* **2006**, *28*, 582 – 586.
[13] D. Ananias, M. Kostova, F. A. A. Paz, A. Ferreira, L. D. Carlos, J. Klinowski, J. Rocha, *J. Am. Chem. Soc.* **2004**, *126*, 10410 – 10417.
[14] P. Dorenbos, *J. Phys. Condens. Matter* **2003**, *15*, 8417 – 8434.
[15] L. van Pieterson, M. Heeroma, E. de Heer, A. Meijerink, *J. Lumin.* **2000**, *31*, 177 – 193.

